Astron. Astrophys. 358, 276–286 (2000)

ASTRONOMY AND ASTROPHYSICS

A novel model for the interpretation of the unidentified infrared (UIR) bands from interstellar space: deexcitation of Rydberg Matter

L. Holmlid

Reaction Dynamics Group, Physical Chemistry, Department of Chemistry, Göteborg University, 412 96 Göteborg, Sweden
(holmlid@phc.chalmers.se)

Received 27 September 1999 / Accepted 5 April 2000

Abstract. The so called unidentified infrared (UIR) emission bands, observed from interstellar space for more than 25 years, are presently believed to be due to carbonaceous material in some form, for example polycyclic aromatic hydrocarbons (PAHs). However, the evidence is based on absorption data, which clearly is not adequate due to differences in the processes, for example the thermal factor. It also seems doubtful that enough carbon is available to form all the required PAHs, and that the vapor pressure is high enough to keep almost all such molecules in the gas phase. We now report on a model in which all UIR bands are due to electronic deexcitation in the condensed phase named Rydberg Matter. This type of very low-density condensed matter is formed by condensation of Rydberg states of almost any type of atom or small molecule, in space mainly hydrogen atoms and molecules. The intial formation of Rydberg states is due to desorption of alkali atoms from surfaces of small particles, especially carbon particles. This desorption can be caused by radiation or moderate heat and gives long-lived circular Rydberg states. Rydberg Matter can be produced in macroscopic quantities in the laboratory. There is no lower gas density limit for its formation. All the reported UIR peaks from different objects fall within the bands for deexcitation from Rydberg Matter states with principal quantum numbers n = 40–200. Most of the transitions are two-electron deexcitation processes, but also one-electron capture processes are identified. The UIR spectra of types A - D can be understood within this model. The agreement with observations is better for the Rydberg Matter model, with small a priori information content, than for the current PAH model.

Key words: molecular processes – ISM: lines and bands – ISM: atoms, ions – ISM: molecules

1. Introduction

The so called unidentified infrared bands (UIR) are observed in emission from interstellar matter, in the diffuse emission from the galactic disk, in a large number of stellar objects, in planetary and reflection nebulae, and in extragalactic sources. At present, a variable mixture of a large number of polycyclic aromatic hydrocarbon (PAH) molecules is often suggested to give rise to these bands. However, there are indications that the amount of interstellar carbon is not sufficient to form all the required PAHs (Dwek 1997). That stable molecules should give rise to this very strong type of bands seems unlikely, since the strongest peak is a factor of 10^3 above the continuous background and the UIR bands are observed almost everywhere in space. If this was the case, many other stable molecules, for example their precursors, would also be expected to show their vibrational emission IR signatures in the same spectral region. Here we instead propose a model where most types of atoms and small molecules take part in the emission from the condensed excited phase named Rydberg Matter (Svensson & Holmlid 1999; Wang & Holmlid 1998).

At least eight broad bands, with half-widths of the order of 0.5–1 μm, are considered to be of the UIR type, with the peak wavelengths ranging from 3.3 to 17 μm. They are of comparable intensities also in different surroundings, and this is one fact which points to a common origin of the bands. Recently, two observed spectra of UIR bands (i.e. emission spectra) were compared in detail with absorption spectra for a large number of PAHs, giving fair agreement (Allamandola et al. 1999). However, all possible gaseous origins for the UIR bands have still not been investigated. Further, the comparison should of course be made with emission data. The reasons for this are several, for example the different absorption and spontaneous emission coefficients, which differ by a factor λ^3, and the thermal populations of the upper vibrational states which differ a factor of 10 for transitions at 5 and 10 μm respectively at 600 K. In the present study, we show that a model of low complexity with fewer input parameters gives good agreement with the observed bands. The source of the UIR bands is proposed to be the general form of matter named Rydberg Matter (RM), which is a phase of matter of the same rank as liquid and solid. The agreement with data is better for this RM model than for other current models.

Rydberg Matter (RM) is a metallic phase of low density, at the lowest densities built up by clusters or sheaths with a thickness of one atomic layer. It is a condensed phase containing any kind of atom or small molecule with interparticle distances of the order of μm. The prediction of RM was made by Manykin et al. (1980). Quite complete quantum mechanical calculations were performed to predict a range of properties (Manykin et al. 1981, 1982, 1983, 1992a,b). The first macroscopic experi-

mental proof was found after 10 years (Svensson et al. 1991; Svensson & Holmlid 1992), and a detailed microscopic proof was presented just recently (Wang & Holmlid 1998, 2000a). RM can be produced in various pressure regimes, and macroscopic amounts of RM can easily be produced at pressures of 1 mbar and at high temperatures, while RM at low pressures and low temperatures useful for microscopic studies is slightly more difficult to produce in the laboratory (Wang & Holmlid 1998, 2000a,b). Since RM is formed by condensation of circular high-Rydberg states, and such states which are formed by recombination of ions and electrons are little disturbed in space at very low pressures, it seems safe to predict that also RM will exist in space in large quantities. This report is part of an ongoing study to search for the signatures of RM in interstellar space, and both the diffuse interstellar bands (DIBs) and the 2.7 K microwave background can be shown to agree well with processes within RM. These results will however be reported separately.

Also events on earth seem to be due to RM. The atmospheric phenomenon named ball lightning is described in several reviews (Singer 1971; Smirnov 1993). The properties of RM agree well with the ones observed for such phenomena (Manykin et al. 1982, 1998). Applications of RM in various devices are in progress, mainly based on the extremely low electron work function of RM surfaces (Svensson & Holmlid 1992).

2. Background

2.1. Rydberg states

Rydberg Matter is a condensed phase of rather weakly interacting long-lived circular Rydberg atoms or molecules. The radiative lifetime of single Rydberg atoms with electrons in circular orbits is large. It increases rapidly with increasing excitation energy and principal quantum number n as n^5, and at n = 100, it reaches 100 ms. The long lifetimes are due to the extremely low overlap between the circular states and the lower states. The radiative lifetime for a circular Rydberg atom averaged over the angular momentum quantum numbers is 0.18 s at n = 40 and 17 s for n = 100 (Beigman & Lebedev 1995). The diameter of Rydberg atoms varies as n^2, being 170 nm at n = 40 and 1.06 μm at n = 100 (see Stebbings & Dunning 1983; Gallagher 1994 for general information on Rydberg states).

2.2. Formation of RM

In space, energetic particles and quanta ionize atoms and molecules, and the consecutive recombination processes with free electrons will initially form very highly excited Rydberg, thus very long-lived circular states. The long radiative lifetimes means that such states are dark, almost not interacting with radiation in the visible or IR ranges. It is well known that Rydberg states with n of the order of 100 exist in space. At a typical density in diffuse ISM of 5x10^7 m^{-3}, a free high Rydberg state with n = 500 will make several collisions during the radiative lifetime of 5x10^4 s, calculated with a rather small cross section of 10^4 nm^2 for Rydberg-Rydberg collisions (Fabrikant 1993). Such Rydberg - Rydberg collisions may be one starting point for condensation. The number of collisions with ground state atoms or molecules will be smaller, due to the much smaller cross sections for such interactions. However, the likely outcome of such collisions which are nearly resonant is excitation energy transfer, and not simply deexcitation. One type of such energy transfer is to ground state clusters, which will then be excited to a Rydberg state. For small clusters, the excitation energy may be large enough to form an RM cluster directly. Otherwise, collisions with further Rydberg states may provide enough energy to transfer the Rydberg cluster to an RM cluster, which will have a much larger radiative lifetime. This is the second possible route to form RM in space.

The third major route to RM formation, which is the one observed to be most rapid in the laboratory, is the desorption of Rydberg states from surfaces by high enough temperature, by visible or more energetic radiation, and possibly energetic particles. Atoms adsorbed on surfaces of carbon or metal oxides, e.g. alkali metal atoms, desorb often thermally directly into Rydberg states (Wang & Holmlid 1998; Holmlid 1998a; Engvall et al. 1999) since the ground state is not stable on the surface (Holmlid 1998c). Circular Rydberg states are formed directly, often in large densities close to the surfaces, and facile condensation to RM clusters with long radiative lifetimes is observed (Wang & Holmlid 2000a). Rydberg atoms at surfaces also directly form Rydberg clusters in the surface sheath bound to the surface (Wang et al. 1999). In subsequent collisions between the desorbing Rydberg atoms (or clusters) and gas atoms and molecules outside the surface, transfer of excitation energy is possible, as observed in the formation of RM clusters of H_2 and N_2 at metal oxide surfaces in ultrahigh vacuum (Wang & Holmlid 2000b). In such cases the initially desorbed Rydberg atom or cluster, in space maybe mainly alkali or hydrogen Rydberg atoms, will act as a kind of catalyst for the formation of Rydberg states also of small molecules. The mechanisms involving surfaces of interstellar particles of carbon or other nonmetal surfaces are the most likely ones to form Rydberg Matter in the ISM. This means that there is no limit in the gas phase density, below which the RM forming processes can not operate. On the contrary, the lower the temperature and the gas density is, the slower are competing processes, which will tend to increase the formation of RM.

One further possibility to desorb Rydberg states is by photons absorbed by particle surfaces. Photons with rather low energy may desorb alkali metal atoms into Rydberg states from carbon and metal oxide surfaces (Wang & Holmlid 1998, 2000a,b). The same process should also be possible to form Rydberg atoms of H. Wavelengths of 560–570 nm (2.2 eV energy) were used to cause Rydberg state desorption from surfaces at room temperature by stray laser light, but no studies were made of the wavelength dependence over a larger range. It is also likely that carbonaceous and similar small particles will absorb radiation in the visible and NIR quite efficiently. In general, the simplest process to form Rydberg states rapidly in the laboratory is to heat a carbon or metal oxide surface with some alkali metal impurities to $T > 1200$ K (Holmlid 1998a). Thus, a mild

heating even by NIR and visible photons in space with a typical radiation temperature of > 1200 K should give desorption of Rydberg states and RM formation. Otherwise, a more energetic radiation may give direct desorption of Rydberg states to form RM at lower temperatures. The limiting requirement here may be that the temperature of the carbon or metal oxide particles is high enough to allow diffusion of hydrogen or alkali atoms in the bulk.

Thus in the laboratory, it is sufficient to heat a graphite or other surface with a graphite layer, or a metal oxide surface, to rapidly form Rydberg states of alkali metal impurities, which then condense to form Rydberg clusters and RM clusters. A rather low intensity visible light is also shown to desorb Rydberg states and to form RM. These states also have catalytic effects and transfer their energy to gas molecules to form Rydberg states and RM. It is likely that the same processes take place in the ISM at particle surfaces at much lower temperatures, since the quenching rate of the Rydberg species is lower due to the much lower density.

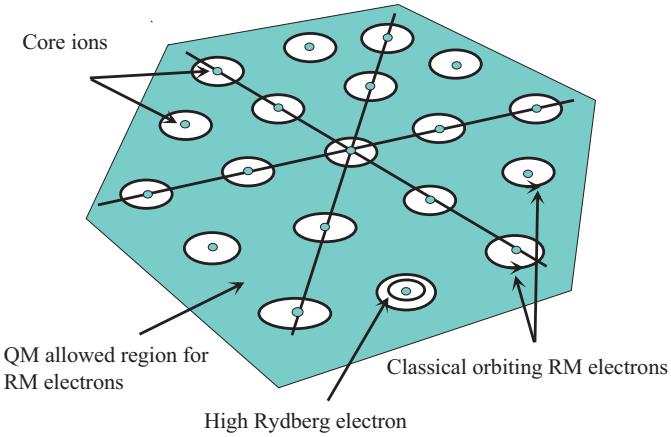

Fig. 1. A perspective view of a cluster of Rydberg Matter with 19 atoms or molecules. The core ions in interstellar space will in general be H^+ and H_2^+, with one electron per atom or molecule excited to the RM region. The core ions giving the two-electron UIR bands must however contain at least one excitable electron.

2.3. Electronic structure in RM

RM is a condensed matter with good electronic conductivity. Thus, it is similar to a metal in its properties. The conduction band contains the excited electrons and is half-filled as for ordinary metals. Within the phase of RM, the bare ions M^+ are surrounded by the electron cloud which forms cavities in which the ions reside. The work function of RM is very low, of the order of 0.1 eV at large excitation levels (Holmlid 1998b), while the bottom of the conduction band is at approximately twice this value below the ionization limit. This means that RM at not too low temperatures is a very good electron emitter, which may give charging of adjacent atoms and molecules, even of Rydberg states to form excited negative ions of e.g. hydrogen (Pinnaduwage et al. 1999).

It is necessary to determine the excitation state, and thus the width of the conduction band to know the electronic state of RM in space. For high density RM, electron emission experiments give work functions down to 0.4 eV (Holmlid & Manykin 1997), but similar measurements for low density RM are not possible. Laser Raman experiments give higher excitation levels for dense RM, corresponding to $n > 55$ (Svensson & Holmlid 1999). Recent interpretation studies of DIB lines in the ISM give an average value under such conditions of n = 80–90 (Holmlid 2000). In cold regions of the ISM, even higher values of n are likely.

It is predicted from theory that a stable phase of RM will not absorb or emit in the visible, and that there will exist an absorption edge in the IR. At the likely excitation level of $n > 50$ in space, this absorption edge will be moved very far away, probably into the cm wavelength range. In the laboratory, RM does not absorb or radiate in the visible range even in macroscopic quantities at high temperatures. Thus, stable RM will transmit almost all quanta in the visible and IR without interacting with them.

2.4. Clusters of RM

Laser induced fragmentation of RM clusters (Wang & Holmlid 1998) gives a clear microscopic proof of the shape of such clusters. Depletion experiments show that the clusters contain 7, 14, 19, 37, and 61 atoms. These numbers are called the magic numbers for the most stable cluster forms, and they do not agree with the magic numbers for spherical clusters. Instead, they are characteristic for planar closepacked (hexagonal) monolayer clusters. The cluster form with 14 atoms is interpreted as a dimer of the basic cluster with 7 atoms. Since the electron in a circular Rydberg state moves quite accurately in a planar circular orbit, a picture with all the electrons in an RM cluster moving in one plane emerges. Classical calculations including correlation effects show that this is indeed the case (Holmlid 1998b). Work functions and binding energies were calculated in reasonable agreement with the previous QM calculations due to Manykin et al. (1992a). The very high quantum numbers involved means that a classical description of the electron motion should be possible, which is found to be correct for many processes involving Rydberg states (Wang & Olson 1994). A classical electron in RM moves in a circular orbit around its core ion, which means that it has both a large principal quantum number n and a large angular momentum quantum number l. The electron motion takes place in a plane, and if bonding shall exist, all the highly excited electrons have to move in one plane (Holmlid 1998b). Thus, RM has the form of planar monolayer of atoms. A view of a 19-atom or 19-molecule cluster of RM is shown in Fig. 1. There exist some effects which will prevent the formation of stable RM sheaths with hundreds of atoms or more, namely the retardation effects due to the finite propagation speed of light. This means that the electron motion will not be synchronous for very large clusters, and that the binding forces in the RM sheaths will be weakened (Holmlid 1998b).

2.5. Chemical composition of RM

It is important to realize that the RM structure will be the same independent of which atom or molecule it is built up from, as long as the internal degrees of freedom in the molecules do not couple directly to the excited electrons in the RM, or the molecule is too large to be accommodated into the RM structure. This means, that even if most experiments to date have been made with alkali metals due to the simplicity of forming such RM, any atom (especially hydrogen) can replace the alkali atoms in RM. In some experiments referenced here, the special features of the various atoms and molecules in RM are used to extract information about RM: this would certainly be much harder to do if the RM in the laboratory was built up only from H atoms. Thus, the information on the RM structure and properties is believed to be very general, even if each system studied experimentally has its own special features. Studies similar to the ones on alkali RM clusters have also been done with RM clusters formed by small gas molecules, like N_2 and H_2 (Wang & Holmlid 2000a,b). The formation of H_2 (RM) is of course of great interest in relation to RM formation in space.

2.6. Bond distances in RM

Both the classical and QM calculations on RM gives a simple relation between the excitation level of RM and the bond distances between the core ions in the RM. At the excitation level of n = 80 likely to be approximately valid for most of the ISM due to the interpretation of the so called DIB lines as caused by RM (Holmlid 2000), the interionic bonding distance is 1 μm. At n = 55, the distance is slightly smaller, namely 500 nm. These quite large distances have not yet been measured in the laboratory, probably due to too rapid quenching by molecules incorporated into the RM and to residual gases in the vacuum chambers used. Further, the energy spread due to thermal initial energy is too large to make it possible to observe the expected small kinetic energy releases in laser fragmentation experiments. So far, laser induced Coulomb explosions in RM clusters indicate a bonding distance of 4–6 nm giving an energy release of 0.2–1.0 eV.

2.7. Lifetime of RM

Manykin et al. also calculated the lifetime of RM in different excitation levels, and found it to be long, of the order of 100 years at an excitation level of n = 16. The main deexcitation processes for RM were found to be Auger processes (Manykin et al. 1992b), involving two electrons which simultaneously change their energy and orbital angular momentum. At n = 80 which may be correct for the ISM, the lifetimes from a simple extrapolation would be extremely large according to this calculation, longer than the lifetime of the universe. Of course, the background radiation of a few K temperature will interact with RM and possibly shorten the lifetime, an effect which is well documented for isolated Rydberg atoms (Gallagher 1994). Other external interactions like energetic particles and quanta will disturb the RM even stronger, and internal interactions like coupling to molecular rotation in RM will shorten the lifetime drastically.

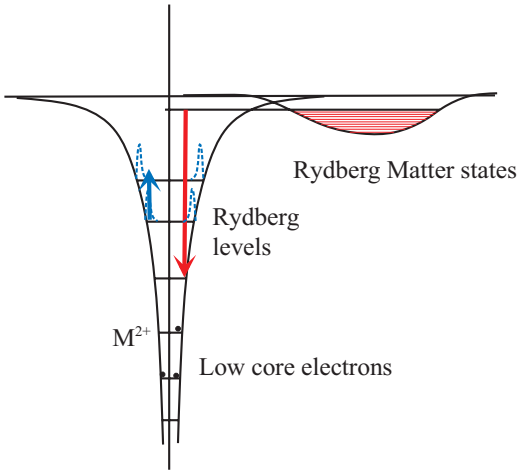

Fig. 2. Emission of light from RM by the two-electron mechanism, Eq. (2), in which one electron falls down from the RM Fermi level to an intermediate Rydberg state at the same time as another electron is excited from one Rydberg state to another, higher one.

3. Deexcitation of Rydberg Matter

The electrons which are excited into the partly delocalized orbitals in RM also give the bonding between the atoms in RM, as in an ordinary metal. The various energy levels for the core level electrons close to the core ions, the RM electrons in the conduction band between the atoms, and the empty intermediate electronic states around the core ions are shown in Fig. 2. The conduction band is approximately half-filled, and the energy required to move an electron from the highest occupied orbital in the conduction band (at the Fermi level) to infinite distance is the surface work function. This energy is small, of the order of a few K at excitation levels of n = 80.

A direct deexcitation process

$$\mathrm{M}^+ + \mathrm{e}^-_{RM} \rightarrow \mathrm{M}(nR) + h\nu \qquad (1)$$

with emission of a photon corresponding to the energy difference between a level in the RM continuum and a rather low Rydberg state in the atom or molecule M is not very likely due to the very small overlap between these states. However, if electrons are released in the RM by for example energetic particles, or a free electron current passes through the RM due to external accelerating fields, a direct capture of this type may take place. The final state is indicated as nR, which means a Rydberg electron with principal quantum number n and maximum angular momentum quantum number l. There is no selection rule for the n value, but a selection rule for the angular momentum quantum number l must exist, with the change $\Delta l = \pm 1$. This process is a deexcitation process for RM, since the final result is a Rydberg atom or molecule separated from the RM. It is the simplest process giving transitions of relevance to the UIR bands, but a slightly more complex process is also likely, as shown below.

Two-electron processes are observed in laser Raman spectroscopic experiments in RM (Svensson & Holmlid 1999). This means that when one electron falls down from the RM states, a Rydberg electron in the same atom is excited slightly with a simultaneous large change in the value of l. The complete process may then be written

$$\mathrm{M}^+(n_1 l_1) + \mathrm{e}^-_{RM}(n_2 l_2) \rightarrow \mathrm{M}(n_3 l_3; n_4 l_4) + h\nu \qquad (2)$$

where l_1 +l_2 - l_3 - l_4 = ± 1 should be valid. This process is depicted in Fig. 2. The main contribution to the emitted light would come from the energy change from the RM level at n_2 to a low value n_4 of one electron. The energy change from a high value n_1 to another relatively high value n_3 may be rather small, since the Rydberg energy levels vary as n^{-2} relative to the ionization limit. This kind of process also implies a deexcitation of the RM, since the final state is a neutral atom or molecule, albeit in a doubly excited state. Of course, this type of process can only exist if the central core in the M atom or molecule has at least two charges, which excludes H atoms. Hydrogen molecules on the other hand may take part in such a process, but may suffer dissociation after the electron transfer is completed.

The RM surviving for a long time at high n values in the range n = 50 - 90 and large binding distances, 0.4–1.2 μm, may finally deexcite by sequential emission of many IR quanta to lower RM states to which the overlap has increased above some minimum value. This means, that the IR transitions to the low n values may take place from upper states with a lower state of excitation than for radiative transitions to not so low n values.

4. Results

There exist good surveys over the UIR bands in the literature (Tokunaga 1997, Geballe 1997) and several other recent studies, like the ones taken with SWS onboard the ISO. The values found for the various peaks of the spectra are collected in Table 1, using the UIR spectral classification schemes from the UIR surveys. Note that the peaks observed are not very sharp, with typical FWHM of 0.05–0.5 μm depending on the wavelength range and the astronomical object. In Table 1, the values given in the publications as the peaks of the broad bands are collected. These peaks are found in different objects, and it should be noted that all these peaks for one band are not found in the same object.

The energy changes following the deexcitation from the RM to a relatively low nR state as in Eqs. (1) and (2) can easily be calculated from the Bohr formula. In the case of the process in Eq. (2), the final state for the electron in a state with quantum number n_4 is the second highest in the atom. Thus, a double charge on the core ion must be used to take into account that the final state is a low Rydberg level, inside the orbit of the highest electron ending up in state $n_3 R$. In Table 1, the transitions in M and M^+ matching the observed peaks are given. It is seen that the observed features fall into bands, which are limited towards short wavelengths by a transition from a very high n number around n = 200 to a certain lower n number, between 10 and 22 for most of the bands. This means that there exists a type of band heads at the wavelengths 3.29, 3.87, 4.49, 5.16, 5.87, 6.64, 7.45, 8.30, 9.21, 10.16, and 11.17 μm. Just a few of these low wavelength limits have been observed directly, but the largest UIR peaks which correspond to transitions from $n \approx 60$ are just above these values, like 3.3–3.4, 4.6, 5.6, 6.2, 6.9, 7.6, and 11.5 μm. Each band is limited towards long wavelengths by a transition from the lowest stable RM state, of the order of n = 50 (Svensson & Holmlid 1999). The most apparent such peaks are normally 3.53, 5.6, 8.59, 10.4 and 12.7 μm, which correspond to RM excitation states of n = 45, 51, 48, 57 and 60 respectively. These values increase with the lower n value (n = 12, 15, 18, 20 and 22), which is reasonable if the overlap between the two states is considered. It is easily seen that all the observed UIR peaks fall within these bands. The differences in the spectra between different objects and spectral types A - D are believed to be due to real differences in the conditions of the RM. This will be discussed below.

The possible transitions from RM levels down to states in M^+ or M thus fall within broad bands, as shown in Table 1. The actual peaks observed in any object must lie within these bands, and that is the case for all observed peaks. However, the actual peak observed in any object is due to the excitation state and other parameters like the density of the RM phase, and can not be predicted at present. The short wavelength limits of the bands can be predicted quite accurately. For example, if the RM level would be n = 300 instead of 200 as in Table 1, the wavelength at 5.16 μm would shift very slightly to 5.14 μm. The long wavelength limit is however more uncertain: a change from n = 46 to 50 for the 6.2 μm band means a change in wavelength of the long wavelength limit from 6.63 to 6.50 μm.

A few special features can be observed directly from Table 1. Peaks have been detected for all the bands with lower n = 12–22, with only n = 13 missing (see further in the discussion section). That also so many odd n values are found means that the transitions definitely are in the ions M^+ within the RM. In space, RM is thought to have an excitation level around n = 80, with a lower limit at approximately n = 50. The highest upper level is not known so well, but high excitation levels can only exist at low temperatures due to the low bond strength for high excitation levels. Thus, transitions from n = 200 are considered to correspond to direct electron capture of diffusing electrons within the RM.

To make a detailed comparison with observed UIR spectra, reasonable band shapes have to be used together with band centers from Eqs. (1) and (2). (The observed peak structure interpreted in Table 1 is not used in this case). Since the RM deexcitation bands are expected to be asymmetric (see below), a Gaussian function is not really useful, and a Lorentzian shape is not in agreement with the model assumptions of two-electron processes. Instead, a function similar to a Weibull function is used here, with the form

$$p(\nu, q, t) = \frac{t}{q}\left(\frac{\nu}{q}\right)^{t-1} \exp\left[-\left(\frac{\nu}{q}\right)^{t}\right]$$

which means that the integral over ν from zero to infinity is normalized to unity. Here, ν is used in wave numbers. The peak of this distribution is at q. The parameter determining the width

Table 1. Assignment and classification of the various UIR peaks. Each section of the table indicates one band with transitions from the RM states to an intermediate Rydberg state in M^+ (see the text). The spectral types follow the scheme by Geballe (1997) with some additions due to Tokunaga (1997). The wavelengths where peaks are observed are in bold print. The italicized entries are lower wavelength limits for each band. The transitions 200 $\rightarrow$ for M^+ (100 $\rightarrow$ for M) are considered to be capture of diffusing electrons.

$\lambda(\mu$m)	Transition in M^+	Transition in M	Type of spectra	Refs.
2.77	*200 → 11*			
2.93	45 →			
3.25	Thermal electrons			Beintema et al. (1996)
3.29	200 → 12	100 → 6	A B D	
3.40	65 →		A B D	
3.43	58 →		B C	
3.46	53 →		A B C	
3.53	45 →		A B C	
3.63	39 →			Beintema et al. (1996)
3.87	*200 → 13*			Overlaps with Brα at 4.052 μm
4.20	45 →			
4.49	*200 → 14*	*100 → 7*		
4.6	80 →		A	
4.94	45 →			
5.16	*200 → 15*			
5.24	90 →		A	Roche et al. (1996b)
5.6	51 →		A	
5.87	*200 → 16*	*100 → 8*		
6.01	90 →			Beintema et al. (1996)
6.22	65 →		A B	
6.63	46 →			
6.64	*200 → 17*			
6.9	70 →		B	
7.45	50 →			
7.45	*200 → 18*	*100 → 9*		
7.6	100 →		A	
7.7	90 →		D	
7.8	78 →		A B	
8.0	65 →		B	
8.59	48 →		A A_1	
8.30	*200 → 19*			
8.67	84 →			Beintema et al. (1996)
9.26	57 →			
9.21	*200 → 20*	*100 → 10*		
9.5	100 →			Beintema et al. (1996)
9.7	82 →			Beintema et al. (1996)
10.4	57 →		A	
10.16	*200 → 21*			
11.05	90 →			Beintema et al. (1996)
11.46	60 →			
11.17	*200 → 22*	*100 → 11*		
11.22	160 →		A	
11.3	140 →		D	
11.5	110 →		B	
12.2	71 →		B	
12.73	60 →		A	
13.5	150 → 24			Beintema et al. (1996)
16.4	105 → 26 etc.		A	Moutou et al. (1998)
17.0	200 → 27			Beintema et al. (1996)
21	200 → 30 etc.		B	
30	200 → 36..50		B	

of the skewed function in ν is t. At t = 60, the FWHM of the distribution is +15,-20 cm^{-1} at q = 800 cm^{-1}, and +30,-40 cm^{-1} at 1800 cm^{-1}. This width is reasonable for the simple deexcitations in Eq. (1), while a slightly broader distribution with t = 30 or 20 has been used for the transitions involving also a second electron. In these cases, the distribution for t = 30 has a FWHM of +25,-40 cm^{-1} at q = 800 cm^{-1}, and +60,-80 cm^{-1} at q = 1800 cm^{-1}, and for t = 20 a FWHM of +40,-60 cm^{-1} at q = 800 cm^{-1}, and +100,-130 cm^{-1} at q = 1800 cm^{-1}. (Note that in the PAH model, a Gaussian profile with a FWHM of 30 cm^{-1} is added to each measured absorption line (Allamandola et al. 1999)).

In Figs. 3 and 4 a comparison with two spectra (type A and B respectively) also used by Allamandola et al. (1999) is shown. (Note that the upper scale in the figure in Allamandola et al. is erroneous: the largest peak in Fig. 3 in Buss et al. (1993) is at 12 μm or 830 cm^{-1}, not at 900 cm^{-1} or 11.1 μm as given by Allamandola et al.). The observations are from Buss et al. (1993) and Bregman et al. (1989). The main transitions included are given in the figure captions. The only transitions included in Fig. 4 are such that they correspond to a two-electron process as described by Eq. (2), using intermediate values of RM excitation state (upper level) around 70, increasing with higher n levels for the lower state. The only range where the fit could have been improved substantially is at 8.3 μm, where lower RM states seem to contribute. In Fig. 3 also processes corresponding to electron capture as in Eq. (1) are included in a few sharp peaks, but their total contribution to the signal is very small. Otherwise, just a few transitions are needed to explain the spectrum well. To improve the fits in two band shoulders, small contributions from lower RM states are included in Fig. 3, namely at 8.0 and 12.8 μm.

To compare the goodness of fits between two different models is certainly not trivial. However, the RM model has the added benefit that it is does not use a large a priori information content like the PAH model with its large number of complex spectra. Instead, the RM model assumes only the Bohr formula for the energy levels of Rydberg states. If the PAH spectra could be reduced to a (presumably large) set of parameters, the comparison of the two models could be made on an equal basis. However, in most cases the simplest model, that is the one with the lowest information content, should prevail. The number of simple parameters actually used for the fits of the spectra in Figs. 3 and 4 is 10–12 intensity parameters (contributions above 2%), plus two width parameters. This should be compared to the fits to the PAH model by Allamandola et al. (1999), where 24 intensity parameters (contributions above 2%) are used. The RM model in total comprises 22 parameters in the spectral range in Figs. 3 and 4, while the PAH model (the whole database) comprises 44 parameters (different molecules and ion states). A comparison of the quality of the fits between Allamandola et al. (1999) and the present study shows that the RM model gives considerably better fits to the two observed spectra chosen by Allamandola et al. Thus, both the number of parameters and the required information content in the RM model is considerably smaller than in the PAH model, with better fits.

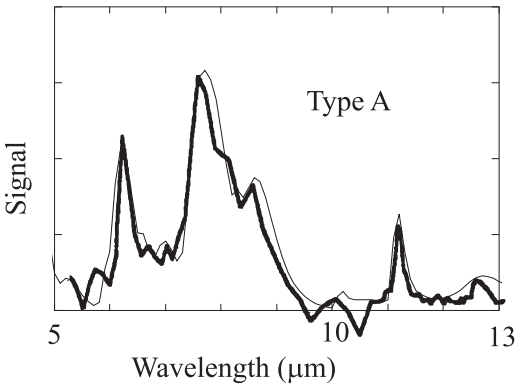

Fig. 3. The best fit of the RM emission model (narrow curve) to the observed data from Orion ionization ridge (broad curve) (Bregman et al. 1989, taken from Allamandola et al. 1999) of spectral type A. The width parameter is t = 35 for most transitions. A width of t = 120 is used for the electron capture process, which is barely significant at n = 16 and 22 ($<$ 2%). The contributions for transitions to the various lower states n is given in percent in parentheses: 14 (29.5), 15 (3.0), 16 (15.9), 17 (5.3), 18 (17.7) and 19 (10.6). Two other contributions are included to take into account transitions to lower RM states (see Table 1) at 8.0 (5.9) and 12.8 μm (5.9). Note that the observed signal is lower than the interpolated background around 10 μm, probably due to foreground absorption.

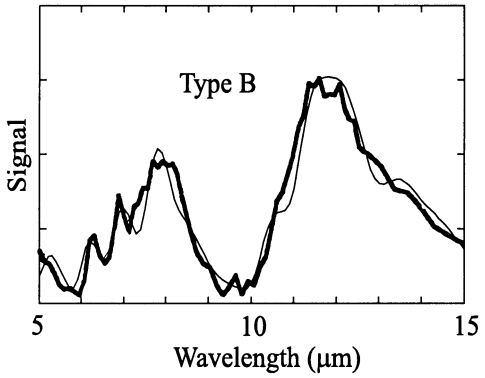

Fig. 4. The best fit of the RM emission model (narrow curve) to the observed data from IRAS 22272+5435 (broad curve) (Buss et al. 1993, taken from Allamandola et al. 1999) of type B. The width parameter is t = 20. The contributions for transitions to the various lower states n is given in percent in parentheses: 14 (10.5), 15 (7.8), 16 (9.2), 17 (11.8), 18 (17.0), 19 (13.9), 21 (7.8), 22 (15.7), 23 (7.8), 24 (5.9) and 25 (2.0).

5. Discussion

The asymmetric broadening observed in the UIR bands is likely due to two effects. The first one is the distribution of the upper excitation level in RM, which should give a broadening of the absorption peaks corresponding to approximately 50 cm^{-1}, or approximately 3% of the wavelength for the range of interest here. This will probably give a slightly asymmetric peak shape, with some tailing to longer wavelengths. The second one is the energy which ends up in the excitation of the second electron involved in the two-electron transition as sketched in Eq. (2). This would give a smaller photon energy, and could thus add

to the observed long slope towards longer wavelengths of the UIR bands. The size of this effect is not known accurately, but a likely transition n = 35 $\leftarrow$ 25 corresponds to slightly less than 100 cm^{-1}, which is of the same size as the half width of most of the UIR bands. Thus, this broadening mechanism is of the correct size. In the study by Allamandola et al. (1999) a broadening was also used, adding a Gaussian with FWHM of 30 cm^{-1} to the measured absorption lines. The reason for this broadening was stated to be intramolecular energy redistribution in the excited PAH molecules.

In both spectra in Figs. 3 and 4, a pronounced minimum exists around 10 μm. The observed signal even becomes negative in Fig. 3, which can be observed as a signal below the average background signal in Bregman et al. (1989). This effect has been attributed to an absorption in foreground silicate (Mattila et al. 1996). Thus, when the fitted spectra show the same minimum, this is due to overfitting. In the RM model, this means that the very low contributions from some of the transitions in this range are false, but this error is simple to correct when data showing the correct behavior around 10 μm become available. However, it is more difficult to correct this in the case of the PAH model. Thus, if this minimum is really due to foreground absorption, the PAH model is at variance with the correct, but not yet measured signal.

In Table 1, the band corresponding to transitions down to n = 13 close to 4.0 μm is missing. As indicated in the table, this transition is probably overlooked due to overlap with the recombination line Brα. In many studies, the range around 4.0 μm is not well covered, due to apparatus limitations and other expected overlaps as well. For example, Beintema et al. (1996) observe absorption bands at 4.2 μm in one of their objects.

The RM model succeeds in explaining all the UIR bands within a simple formula, using the experimental knowledge about RM. Even if the agreement is satisfactory, the astrophysical background and the actual observational details must also agree with the model if it should be trusted. The main characteristic of the UIR is that all the bands and peaks must agree with one type of molecule. The RM model agrees with this limitation, in a better way than other models. Another limitation is the required relation to the carbon concentration in space (Cohen et al. 1989). This connection is very obvious in the case of RM, since the initial atomic Rydberg states are formed during desorption from carbon particle surfaces, as described in Sect. 2.2. Another limitation often mentioned is that the molecules which should be the carrier of UIR must be very stable and should not be destroyed by high temperatures and large fluxes of ionizing radiation. At first sight, such a requirement may seem correct, but an alternative is to require that the UIR carriers should be easily *formed and reformed* at high temperatures and large ionizing fluxes. Since RM is formed by radiation of a small enough wavelength to cause desorption atoms or molecules and by moderate heat, and since it will certainly be reformed over and over again with no complicated dead end in the reaction flux like the PAHs (Allamandola et al. 1989), it seems to be the best choice as the UIR carrier under all circumstances. Note that in the laboratory, heating of a carbon or graphite surface always gives Rydberg states and Rydberg cluster formation of alkali metal impurities, despite the relatively high density of possible quenching gas molecules in the vacuum chambers. Thus, the conditions for RM formation are rather weak and easily fulfilled in space, with no complex reaction schemes for its formation which would imply breaking and forming strong bonds.

For a quantitative comparison of the proposed RM model with observations, both the oscillator strengths for the transitions and the column densities of the emitting particles are needed. Unfortunately, it is not possible at present to predict the probability of the processes proposed in Eqs. (1) and (2), since accurate calculations for deexcitation processes in RM are not yet possible. In fact, ordinary quantum mechanics is probably not sufficient to obtain a reliable picture of the details of the RM structure, but the pilot-wave formulation due to Bohm seems to be required. This description of quantum mechanics can describe the Rydberg states correctly in the classical limit, as shown recently by Carlsen & Goscinski (1999), which ordinary quantum mechanics is incapable of doing. A pilot-wave calculation of RM is quite demanding and has not yet been done. Experimental determinations of the oscillator strengths for the transitions will be attempted in the near future. Column densities may on the other hand be estimated from the assumed density of RM in the emitting clouds, corresponding to 10^6 - 10^{12} m^{-3}, and from the abundances of non-H atoms for the dominating M^+ mechanism in Eq. (2).

In Table 1, the peaks are classified according to the types proposed by Geballe (1997) and Tokunaga (1997). In terms of the peaks observed, the differences between type A and B may not appear large, but the typical shapes in Fig. 3 (type A) and Fig. 4 (type B) show large differences in the intensities of the various peaks. The most obvious difference is that the peaks at 6.2 and 7.6 μm are decreased in type B, while the bands starting at 9.2 and 11.2 μm in Table 1 are much more intense in type B. The reason for this in the RM model is quite simple, since it is only the question of the excitation state and thus also the density of the RM. In type B the transitions start at higher n values than in type A, and thus type B corresponds to a more expanded RM which can only exist if the temperature in the cloud is relatively low. This type of spectrum is usually found in proto planetary nebulas. In type A spectra, the RM is denser, and can exist under the conditions of higher temperatures and larger UV fluxes (Geballe 1997) due to the larger binding energy at the shorter internuclear distances. This corresponds to the most common form of UIR spectra, and it is found for example in planetary nebulas.

The sharp peaks at 3.29 and 11.2 μm in type A spectra indicate transitions from very high n excitation levels in the RM, while it was just concluded that type A spectra correspond to relatively dense RM with a low excitation level. Since these peaks correspond to excitation levels, which are too high to be typical of RM in space, their presence is related to capture of thermal diffusing electrons within the RM. This is also supported by the observation by Tokunaga (1997) that the type A and B spectra are similar but that type A typically show large sharp peaks at 3.3 and 11.2 μm. It should also be noted that such capture pro-

cesses may as well take place as a transition in M: a diffusing electron in RM may have a low angular momentum, and it can then be captured to form M without involving the next highest electron in the core ion M^+ as required for most transitions in Table 1.

One further observation from Table 1 is that it is only at 3.29 μm and at the long wavelength bands from 11.2 μm that this type of transition from a very high upper n value is observed. Such transitions are of course expected for electrons within the RM for the long wavelength transitions, since there will exist an overlap for such transitions. However, in the case of transitions to lower states, the overlap is expected to be very small, and thus the capture of diffusing electrons may be most important in the case of the 3.29 μm peak. In two objects a peak at even shorter wavelengths was observed (Beintema et al. 1996). This value, 3.25 μm is too small to come from even the ionization limit in the RM. Instead, it must correspond to capture of diffusing electrons, in this case of free electrons with an excess energy of 0.04 eV above the ionization limit. This kinetic energy corresponds to a temperature of 460 K, and this does not appear unrealistic for these proto planetary and planetary nebulae.

The very accurate measurements by Beintema et al. (1996) and Molster et al. (1996) give further results which support the RM model. Molster et al. point out that some strong peaks shift by as much as 0.05–0.18 μm between the proto planetary and planetary nebulae. These peaks are in the middle of the bands in Table 1. The shift may in itself be too small to give any precise information, but Molster et al. also note that other peaks such as 3.29, 6.01, 7.60 and 11.04 μm are stable. These peaks are seen by reference to Table 1 to lie almost at the short wavelength limit in their respective bands, and they can thus not change considerably since these limits are fundamental, not dependent of the exact conditions in the RM. This evidence is strongly in favor of the RM model.

Also in the study by Roelfsema et al. (1996) using ISO-SWS, there is very clear evidence of some of the less often observed bands and peaks. For example, the transitions RM $\rightarrow$ 21 are observed clearly peaking at 11.04 μm. Also, the 8.6 μm peak is shown to vary independent of 7.7 μm. As seen in Table 1, these observations agree well with the expected peaks for the RM model.

There exist two further spectral types, namely type C, which is found in only three sources according to Tokunaga (1997), and type D, which is found in two novae according to the classification by Geballe (1997). Type C shows a prominent peak at 3.53 μm, even larger than the peak at 3.2 μm. The objects showing type C spectra are slightly obscured young stellar objects in dark clouds. From Table 1, the peak at 3.53 μm indicates a very dense RM with a low excitation level, presumably due to large densities and relatively high temperature. This seems to agree with the conditions close to a young star. Type D spectra are similar to type B in the 3 μm band, thus with no sharp electron capture peaks, but agree better with type A in the 11 μm band. Since only two such novae are known, it is difficult to make a detailed interpretation.

An observation which supports the result most obvious from Table 1, namely that all the observed peaks fall within certain bands, is the one given by Roche et al. (1996a). It is shown by the authors that the peaks at 3.4, 5.25 and 11.25 μm have the same shape. From Table 1, these three peaks are close to the limit of large n, which is reasonable due to their similar shapes. All three bands have the same width, namely 50–60 cm^{-1}, corresponding to the distance from n = 200 down to n = 80. The excitation level n = 80 is the most likely upper level of the ordinary RM in space, as also concluded from data on the diffuse interstellar bands (DIBs) (Holmlid 2000). This supports the interpretation in terms of the RM model.

In Table 1, the three last entries correspond to the broader features observed in some objects. The final one, the broad band with its peak at 30 μm (Justtanont et al. 1996, Omont et al. 1995), is proposed to be due to transitions from very high excitation levels or by capture of diffusing electrons down into the lower RM states, not into atomic or ionic states. This may also explain its slightly different, more symmetric shape.

One of the objects studied by Beintema et al. (1996) and Molster et al. (1996) is HR4049, which is a proto planetary nebula. It may be classified with a type C spectrum. This spectrum contains some rather unusual UIR peaks, like 3.25, a large 3.53, 6.01, 8.67, 9.7, 11.05 μm which provide evidence for some of the not so often observed bands in Table 1. It is interesting that it is in these very young stellar objects that all the RM bands appear, while older objects show type A spectra, with just a few of the bands preserved. This may indicate that the ISM is in RM form, and that the star formation with strong UV radiation destroys most of the RM material or the carbon particles required for RM formation. The typical sharp peaks in type A spectra are probably partly due to electron capture of diffusing electrons, and this may indicate that many charged particles reach the RM in type A objects. Thus, the typical type A objects are depleted in their UIR characteristics due to the strong radiation and do not show the full richness of transitions found in the younger objects.

A very interesting study with spatial resolution of the IR emission in one object is reported by Sloan et al. (1993). It is shown that no UIR peaks are observed in the center of the object HD 44179. At about one arcsec from the center, peaks at 7.9 ("7.7"), 8.6, 11.3 and 12.7 μm suddenly appear with relative intensities in this order, and then decay further out. The authors interpret their observations within the PAH model, but the RM model may fit the results even better. RM is formed from hydrogen and other gases at some distance from the object where the temperature and density has fallen enough. Further out, the RM becomes less dense and colder, thus the excitation level is higher giving a more expanded RM. The observed peaks according to Table 1 correspond to transitions 70 $\rightarrow$ 18, 84 $\rightarrow$ 19, 140 $\rightarrow$ 22 (or 70 $\rightarrow$ 21) and 60 $\rightarrow$ 22. That the intensity of the 7.7 μm peak drops more quickly than the longer wavelength peaks is expected, since the RM will occupy higher states further out, giving less overlap to low states. The 7.9 μm peak also changes to 7.4 μm further out, which may indicate mainly electron capture at long distance from the center, and the 11.3 μ m peak has

an intermediate maximum at some distance from the center of the object, which may indicate that 70 → 21 and 140 → 22 both contribute. The last one of these should contribute more at longer distance, since it corresponds to large excitation levels.

Similar studies with spatial resolution of the UIR bands have also been made on galaxies, for example by Metcalfe et al. (1996) on the dwarf galaxy Haro 3. They show maps of emission in the ranges 7–8.5 μm and 12–18 μm, as well as a ratio map of the intensities in these two spectral ranges. Several UIR peaks are observed, most of them indicating RM of low density and no capture processes, which of course will be unlikely to be observed in such an extended object. The maps of the IR emission are very similar to the Hα light maps, which agrees with the description that the RM mainly contains hydrogen. The ratio map shows that the emission around 7.7 μm is stronger in the inner parts of the galaxy, which is the same feature as described above for a much smaller object, caused by the higher excitation level of RM at lower temperature and lower densities further out in the galaxy.

A comparison of peak heights in Mattila et al. (1996) shows that the ratio between the peaks of the 11.3 and 7.7 μm bands is constant for different astronomical objects, while the ratio between the peaks at 6.2 and 7.7 μm is considerably smaller in the emission from the galactic disk. By reference to Table 1 one can conclude that the 6.2 μm peak is due to a transition from a rather low excitation level n = 65. In the galactic disk, the radiation field should be relatively low, and the density and temperature should be low as well. Thus it is likely that the long-lived states at high excitation levels should be more populated, and thus that transitions with longer wavelengths are more probable, which agrees with the observations.

There also exist studies which correlate the UIR band strength to the FIR (far-IR) intensity measured in the range of 100 μm wavelength (Onaka 1997). A very good correlation is found. This is of course difficult to understand if two different types of particles give these contributions, and even more so if PAH gives the UIR bands and small silicate particles give the FIR radiation. From Dwek (1997) it seems that it is not obvious which particle type gives the main contribution at 100 μm. If RM is also the main emitter giving the FIR intensity, the correlation is obvious.

6. Conclusions

It is shown that good agreement with spectra of the so called unidentified infrared emission (UIR) bands is found for the calculated emission due to electronic deexcitation from Rydberg Matter. The electronically excited Rydberg Matter can incorporate any atom or small molecule, and it is formed at carbon or other particle surfaces at low pressure under the influence of moderate heat and photon fluxes. All the observed peaks fall within bands corresponding to transitions from RM states between principal quantum number n = 40 and 200. The transitions go down to a relatively low level with n = 12–22 in a core ion in the Rydberg matter, i.e. the transition involves also the next highest electron in an atom or a molecule as for example H_2 or Na. Also transitions where the core ions capture diffusing electrons exist. The agreement with the examples of type A and B spectra used by Allamandola et al. (1999) is improved in the RM model compared to the PAH model used by these authors. Other recent observational evidence also provides support for the RM model.

Acknowledgements. My sincere thanks to the Referees on this manuscript. Without their helpful advice to a newcomer to the field, the results would not have reached their present form. This study has been partly supported by the Swedish Research Council for Engineering Sciences.

References

Allamandola L.J., Hudgkins D.M., Sandford S.A., 1999, ApJ 511, L115
Allamandola L.J., Tielens A.G.G.M., Barker J.R., 1989, ApJS 71, 733
Beigman I.L., Lebedev V.S., 1995, Phys. Reports 250, 95
Beintema D.A., van den Ancker M.E., Molster F.J., et al., 1996, A&A 315, L369
Buss R.H. Jr., Tielens A.G.G.M., Cohen M., et al., 1993, ApJ 415, 250
Bregman J.D., Allamandola L.J., Tielens A.G.G.M., et al., 1989, ApJ 344, 791
Carlsen H., Goscinski, O., 1999, Phys. Rev. A 59, 1063
Cohen M., Tielens A.G.G.M., Bregman J., et al., 1989, ApJ 341, 246
Dwek E., 1997, PASPC 124, 121
Engvall K., Kotarba A., Holmlid L., 1999, J. Catal. 181, 256
Fabrikant I., 1993, Phys. Rev. A 48, R3411
Gallagher T.F., 1994, Rydberg Atoms. Cambridge University Press, Cambridge
Geballe T.R., 1997, PASPC 122, 119
Holmlid L., 1998a, Chem. Phys. 230, 327
Holmlid L., 1998b, Chem. Phys. 237, 11
Holmlid L., 1998c, J. Phys. Chem. A 102, 10636
Holmlid L., 2000, J. Phys. B submitted
Holmlid L., Manykin E. A., 1997, J. Exp. Theor. Phys. JETP 84, 875
Justtanont K., Barlow M.J., Skinner C.J., et al., 1996, A&A 309, 612
Manykin É.A., Ozhovan M.I., Poluéktov P.P., 1980, Sov. Phys. Tech. Phys. Lett. 6, 95
Manykin É.A., Ozhovan M.I., Poluéktov P.P., 1981, Sov. Phys. Dokl. 26, 974
Manykin É.A., Ozhovan M.I., Poluéktov P.P., 1982, Sov. Phys. Tech. Phys. 27, 905
Manykin É.A., Ozhovan M.I., Poluéktov P.P., 1983, Sov. Phys. JETP 57, 256
Manykin É.A., Ozhovan M.I., Poluéktov P.P., 1992a, Sov. Phys. JETP 75, 440
Manykin É.A., Ozhovan M.I., Poluéktov P.P., 1992b, Sov. Phys. JETP 75, 602
Manykin É.A., Ozhovan M.I., Poluéktov P.P, 1998, J. Moscow Phys. Soc. 8, 19
Mattila K., Lemke D., Haikala L. K., et al., 1996, A&A 315, L353
Metcalfe L., Steel S.J., Barr P., et al., 1996, A&A 315, L105
Molster F.J., van den Ancker M.E., Tielens A.G.G.M., et al., 1996, A&A 315, L373
Moutou C., Sellgren K., Leger A., et al., 1998, PASPC 132, 47
Omont A., Moseley S.H., Cox P., et al., 1995, ApJ 454, 819
Onaka T., 1997, PASPC 124, 170
Pinnaduwage L.A., Ding W.X., McCorkle D.L., et al., 1999, J. Appl. Phys. 85, 7064

Roelfsema P.R., Cox P., Tielens A.G.G.M., et al., 1996, A&A 315, L289
Roche P.F., Lucas P.W., Geballe T.R., 1996a, MNRAS 281, L25
Roche P.F., Lucas P.W., Horae M.U.G., et al., 1996b, MNRAS 280, 924
Singer S., 1971, The Nature of Ball Lightning. Plenum, New York
Sloan G.C., Grasdalen G.L., LeVan P.D., 1993, ApJ 409, 412
Smirnov B. M., 1993, Phys. Reports 224, 151
Stebbings R.F., Dunning F.B., 1983, Rydberg States of Atoms and Molecules. Cambridge University Press, Cambridge
Svensson R., Holmlid L., 1992, Surf. Sci. 269/270, 695
Svensson R., Holmlid L., 1999, Phys. Rev. Lett. 83, 1739
Svensson R., Holmlid L., Lundgren L., 1991, J. Appl. Phys. 70, 1489
Tokunaga A.T., 1997, PASPC 124, 149
Wang J., Holmlid L., 1998, Chem. Phys. Lett. 295, 500
Wang J., Holmlid L., 2000a, Eur. Phys. J. D. submitted
Wang J., Holmlid L., 2000b, Phys. Chem. Chem. Phys. submitted
Wang J., Olson R.E., 1994, Phys. Rev. Lett. 72, 332
Wang J., Engvall K., Holmlid L., 1999, J. Chem. Phys. 110, 1212